Available online at www.sciencedirect.com
ScienceDirect
C. R. Physique 10 (2009) 167–175
COMPTES RENDUS PHYSIQUE

Laser acceleration of particles in plasmas / Accélération laser de particules dans les plasmas

Laser electron acceleration with 10 PW lasers

Luis O. Silva [a,*], F. Fiúza [a], R.A. Fonseca [a], J.L. Martins [a], S.F. Martins [a], J. Vieira [a], C. Huang [b], W. Lu [b], F. Tsung [b], M. Tzoufras [b], W.B. Mori [b]

[a] *GoLP/Instituto de Plasmas e Fusão Nuclear, Instituto Superior Técnico, Lisbon, Portugal*
[b] *University of California Los Angeles, Los Angeles, USA*

Available online 25 April 2009

Abstract

The development of new laser systems, in the 10 PW range, will push Laser Wakefield Accelerators (LWFA) to a new qualitative regime, where different configurations, approaches, and parameters can be explored. Based on the design parameters to be expected for some of these systems (e.g. the future Vulcan 10 PW OPCPA laser system), we have explored the optimal parameters for a single LWFA stage, using the theoretical scalings for these parameters (pulse duration ≈ 30 fs, energy ≈ 300 J). The scalings predict the possibility to accelerate electron bunches to energies close to the energy frontier, with self-injected electrons in excess of 10 GeV, and above 50 GeV bunches with externally-injected electrons. We have used these parameters as a baseline for 3D full scale simulations, confirming self-guiding of 10 PW lasers over distances in excess of 10 cm, and 12 GeV self-injected beams, in agreement with theoretical predictions for the maximum energy gain and the injected charge. In externally guided configurations, our simulations confirm the accelerating gradients and the stability of the laser guided propagation for the long distances required to reach the energy frontier. ***To cite this article: L.O. Silva et al., C. R. Physique 10 (2009).***

Résumé

Accélération laser d'électrons avec des lasers 10 PW. Le développement de nouvelles installations laser, dont l'échelle de puissance atteint le petawatt, vont permettre aux accélérateurs plasma (LWFA) l'accès à des régimes qualitatifs inédits, où différents paramètres et configurations pourront être testés. A partir des données prévues pour de telles installations (i.e., le prochain laser Vulcan 10 PW OPCPA), nous avons recherché les paramètres optimaux dans le cas d'un accélérateur plasma à un étage, utilisant les lois d'échelles existantes pour ces paramètres (durée de l'impulsion = 30 fs, énergie = 300 J). Les lois d'échelles prédisent l'accélération de paquets d'électrons à des énergie proche de l'énergie frontière, 10 GeV pour des électrons auto-injectés et au delà de 50 GeV pour des électrons injectés. Ces paramètres définissent un cadre de travail pour des simulations numériques 3D à pleine échelle qui confirment l'auto-guidage de lasers 10 PW sur des distances supérieures à 10 cm et l'accélération de faisceaux auto-injectés au delà de 12 GeV. Ces résultats corroborent les prédictions théoriques de la charge injectée et du gain d'énergie maximal. Dans le cas de configurations à guidage externe, nos simulations se révèlent être en accord avec les gradients d'accélération et avec la stabilité de propagation du laser guidé sur de longues distances, nécessaires pour atteindre l'énergie frontière. ***Pour citer cet article : L.O. Silva et al., C. R. Physique 10 (2009).***

Keywords: Laser; Plasma; Acceleration

* Corresponding author.
E-mail address: luis.silva@ist.utl.pt (L.O. Silva).

1631-0705/$ – see front matter
doi:10.1016/j.crhy.2009.03.012

Mots-clés : Laser ; Plasma ; Accélération

1. Introduction and motivation

The next generation of laser systems that are now being planned all over the world will deliver powers in excess of 10 PW, with a OPCPA configuration (e.g. the upgrade for the future Vulcan 10 PW OPCPA system [1]), pulse durations in the 30 fs range, and pulse energies in the 300 J range. These conditions will enable the exploration of new scenarios for electron acceleration in Laser Wakefield Accelerators (LWFA) [2]. The available energy in these laser pulses will allow for the exploration of LWFA in the strongly relativistic regime, with peak intensities in excess of $\approx 10^{24}$ W/cm^2, LWFA with moderate relativistic intensities $\approx 10^{19}$ W/cm^2, or even in the weakly relativistic regime $\lesssim 10^{18}$ W/cm^2. Phenomenological models [3–5], and numerical simulations [6–8] will play a critical role in this process, by providing deeper insights on the physical processes involved and standing as an effective tool for the design of the experiments. Experiments [9–13] and simulations [5,14] with laser parameters up to 1 PW have already demonstrated monoenergetic beams, with energies that range from a few hundred of MeV up to 1 GeV.

The physical parameters associated with this new generation of LWFA push the envelope of the numerical techniques [6], either from the point of view of the algorithms or from the required computing resources. For instance, the acceleration distance for the optimal parameters predicted by the phenomenological model of Wei Lu et al. [5] is in the scale of 10s cm–10s m, depending on the laser intensity and the corresponding LWFA regime. This is well beyond the current modeling capabilities of standard three-dimensional particle-in-cell (PIC) simulations due to the outstanding computational resources required to model such distances, even using the largest massively parallel computing machines, or due to the numerical issues associated with running PIC simulations with more than 10^6 time steps. Since kinetic processes are critical in the most extreme conditions associated with 10 PW lasers, it is crucial to perform simulations that capture the relevant physics. Possible alternatives to standard PIC simulations can be envisioned: (i) the use of reduced kinetic codes [8,15] which take advantage of the quasi-static approximation [16]; (ii) the implementation of new methods to improve the speed of standard simulations, e.g., performing simulations in a different Lorentz frame [17]; or (iii) the exploration of alternative computational architectures that have the potential of delivering even higher performance, e.g. graphics processors units (GPUs) [18]. On one hand, the use of approximations to simplify the numerical algorithms can be extremely advantageous; for instance, QuickPIC [8] can be more than a thousand times faster than a full PIC code for scenarios relevant to plasma wakefield accelerators and still capture all the relevant physics. On the other hand, the boosted frame scheme, despite several implementation difficulties for LWFA [19], can provide a means to perform the same large scale simulations more rapidly, while keeping all the relevant physics of a standard PIC code.

We leverage on the existing phenomenological models to design numerical experiments in QuickPIC [8], and with the full PIC code OSIRIS [7] (in the laboratory and also in a boosted frame) for the future 10 PW lasers systems, and to identify the expected output parameters of a single stage LWFA in the regime of ultra high intensities [4] and in the regime of moderate relativistic intensities [5], assuming the same set of basic laser parameters. The paper is organized as follows. First, we discuss the optimal parameters for the different LWFA regimes possible with a 10 PW laser system with key parameters similar to systems now being designed (e.g. the Vulcan OPCPA upgrade), from scenarios with self-guiding and self-injection to scenarios associated with external-guiding and external-injection. These scenarios are tested with numerical simulations, with the results including full PIC simulations, with OSIRIS, and reduced simulations, with QuickPIC, for the most computationally expensive regimes. Finally in the last section, we present the conclusions and prospects.

2. Multi-GeV electrons in a single-stage LWFA – 10 PW class lasers

For a given energy and wavelength, different laser powers and intensities will lead to distinct LWFA regimes, with different laser/plasma evolutions and final beam energies. Moreover, the efficiency of energy transfer from the laser pulse to the accelerated electrons is also strongly dependent on laser and plasma parameters. Motivated by recent findings associated with the strongly nonlinear regime [4], we focus our discussion in the bubble or blowout regime, whereby the intensity of the laser propagating in the plasma is strong enough for the laser ponderomotive force to expel the electrons, forming behind the laser a spherically shaped cavity [20], with very good accelerating

and focusing properties [5]. The electrons can either be self-injected or externally loaded in this cavity. For the bubble, or blowout regime, two alternative routes have been proposed in order to design a single LWFA stage, and that can be simultaneously explored with the next generation of intense lasers in the 10 PW range: (i) the laser can be tightly focused to ultra high intensities ($a_0 \gg 10$) propagating in a high density plasma ($n_e \approx 10^{18}$–10^{19} cm^{-3}); or (ii) the laser can be focused to a matched spot-size, corresponding to moderately high intensity lasers ($a_0 \approx 3$–5), and propagate in a lower density plasma ($n_e \approx 10^{16}$–10^{18} cm^{-3}), where a_0 is the normalized vector potential, given by $a_0 \simeq 8.6\lambda_0[\mu\text{m}]I^{1/2}[10^{20}\ \text{W/cm}^2]$, with I the laser intensity and λ_0 the laser central wavelength, and where n_e is the background plasma density. In the first case, the formation of a quasi-monoenergetic peak is associated with the phase-space rotation of the self-injected electrons in the bubble as they reach the dephasing region of the wake [4,14], since in the strongly driven regime the self-injection is continuous. In the second case, phase-space rotation can also operate as a mechanism that leads to the formation of a quasi-monoenergetic spectral feature. Moreover, and since the self-injection process is more moderate for lower a_0, the self-injected electrons can also lead to the shutdown of the injection process, and the formation of localized ultra short monoenergetic beams [14].

The first scenario leads to extreme blowout and the formation of an electron-free bubble [4], favoring strong beam loading and continuous injection, with self-injected charges in the order of tens of nC for a 300 J laser. Since the plasma densities are typically large ($n_e \approx 10^{19}$ cm^{-3}) in this configuration, the accelerating distances are relatively short (a few mm), and the electrons dephase from the accelerating region after gaining a few GeV. In this regime, optimal conditions are associated with the highest possible intensity for a given set of laser parameters [21].

The second regime leads to moderate blowout of the electrons from the axis [5], but guaranteeing proper matching of the laser pump depletion with the dephasing length of the self-injected electrons, thus providing a controllable and well defined acceleration structure of the blowout region. The matching of dephasing and pump-depletion lengths ensures maximum acceleration of the injected particles, and maximum overall efficiency of the process (ratio between the final beam energy – a balance between charge and maximum energy of the electrons in the beam – and the initial energy of the laser) which is inversely proportional to the laser normalized vector potential a_0. However, a_0 still needs to be sufficiently high to guarantee self-guiding ($a_0 \sim 5.8$) [5] and self-injection ($a_0 \sim 3$) [22]. In this regime, the efficiency can be further increased by external injection of an electron beam, and external guiding in a preformed plasma channel, thus relaxing the conditions in terms of a_0. Blowout can still be achieved for $a_0 \simeq 2$, and the restrictions for self-guiding and self-injection no longer need to be guaranteed.

For the second regime, the laser and plasma parameters are determined from the W. Lu et al. phenomenological theory [5]. The model equations can be written as a function of a_0 and laser energy ϵ. In particular, matched laser pulse duration, at full width half maximum (FWHM), τ_{FWHM} to maximize the energy gain, and matched spot size, W_0, to ensure self-guiding, are given by the engineering formulas

$$\tau_{\text{FWHM}}[30\ \text{fs}] \simeq 11.88\left(\frac{\lambda_0[\mu\text{m}]}{0.8}\right)^{2/3}\left(\frac{\epsilon[300\ \text{J}]}{a_0^2}\right)^{1/3} \tag{1}$$

$$W_0[\mu\text{m}] = 13.5\tau_{\text{FWHM}}[30\ \text{fs}] \tag{2}$$

where λ_0 is the laser wavelength. The plasma density, n_{plasma}, and the accelerating length, L_{acc}, that matches the pump-depletion and the dephasing lengths, are

$$n_{\text{plasma}}\left[10^{15}\ \text{cm}^{-3}\right] \simeq 3.71\frac{a_0^3}{P[\text{PW}]}\left(\frac{\lambda_0[\mu\text{m}]}{0.8}\right)^{-2} \tag{3}$$

$$L_{\text{acc}}[\text{m}] \simeq 42.27\frac{\epsilon[300\ \text{J}]}{a_0^3} \tag{4}$$

where P is the laser power.

Estimates for the injected bunch characteristics (energy gain, ΔE, and bunch charge, q) are also provided by this theoretical model, yielding

$$\Delta E[\text{GeV}] \simeq 134.44\left(\frac{\epsilon[300\ \text{J}]}{a_0^2}\frac{0.8}{\lambda_0[\mu\text{m}]}\right)^{2/3} \tag{5}$$

$$q[\text{nC}] \simeq 1.14\left(\frac{\lambda_0[\mu\text{m}]}{0.8}\right)^{2/3}\left(\epsilon[300\ \text{J}]a_0\right)^{1/3} \tag{6}$$

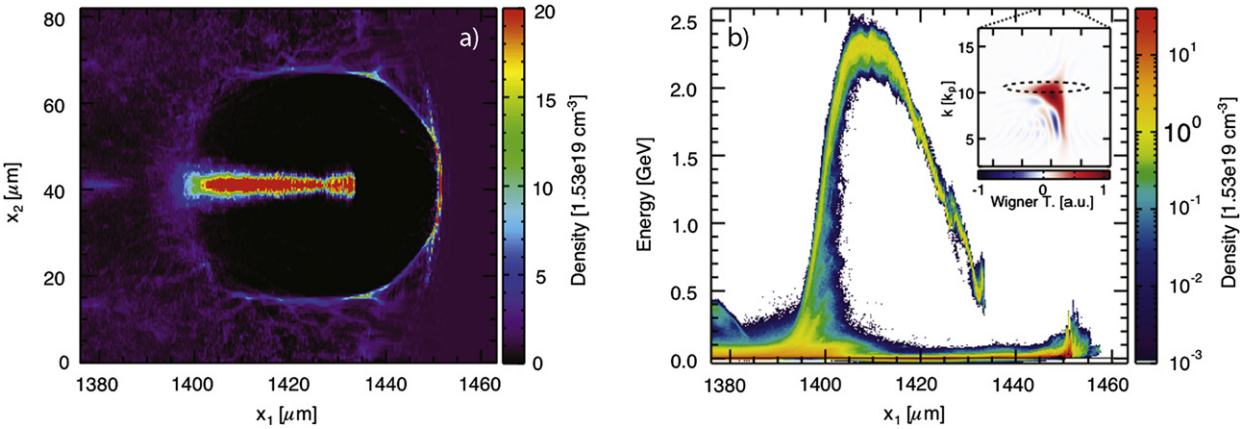

Fig. 1. OSIRIS simulation for the extreme blowout conditions. Slice of the a) electron density across the middle of the simulation window, and b) electron phase-space in the region of the self-injected electrons, with the insert showing the Wigner transform of the lineout of laser field along the propagation direction, with the dashed line representing the region in the Wigner plane of the initial laser pulse.

We observe that Eqs. (1)–(6) include all the relevant numerical factors associated with the phenomenological model, for a linearly polarized laser, and for the matched parameters established by Eqs. (1), (2). When the matched conditions are not satisfied (e.g. in the extreme blowout regime), the full model equations in [5] are still valid and should be used. These scalings provide the parameters to be tested with numerical simulations, and can be used as a guide to the design of the experiments.

3. Numerical simulations

Three-dimensional one-to-one simulations for the three different regimes (extreme blowout, moderate blowout, external injection) were performed with OSIRIS and QuickPIC, with the goal of revealing the physics determining the evolution in the different scenarios, and to estimate the achievable electron beam features. All the simulations have been performed in a moving window, which moves at the speed of light, thus guaranteeing that the laser and the blowout region are always inside the simulation window.

We have considered: (i) the self-guiding/self-injection regime with ultra high intensity laser beams (OSIRIS); (ii) the self-guiding/self-injection regime with moderate intensity lasers (OSIRIS and QuickPIC); and (iii) the external-guiding/external-injection regime with a "low" intensity laser (QuickPIC). For all these regimes, we have determined the optimal conditions predicted by the available models [5,21] for a baseline 10 PW system, assuming that the energy available in the laser pulse is 300 J, while the pulse duration can be compressed down to 30 fs, and the laser spot size can also assume an arbitrary value, within the limits of Gaussian optics.

3.1. Self-guiding and self-injection

In the physical conditions where no external guiding or no externally injected beams are present, the laser dynamics and the interaction with the plasma must guarantee self-guiding, for distances comparable to the dephasing length of the electrons in the wake (which is usually much longer than the diffraction (Rayleigh) length), in order to guarantee maximum efficiency. Furthermore, the accelerated electrons must be trapped, from the background plasma, and self-injected into the bubble-like structure.

For the first scenario, corresponding to the conditions proposed in [4,21], we have considered a 30 fs linearly polarized laser pulse, focused at the plasma entrance with a spot size of 9 μm, corresponding to $a_0 = 43 \gg 1$, propagating in a uniform plasma with electron density $n_{e0} = 1.5 \times 10^{19}$ cm^{-3}. The corresponding simulations were performed in OSIRIS with a $87 \times 82 \times 82$ μm^3 box divided in $3000 \times 256 \times 256$ cells. Given the ultra high laser intensity, mobile ions were used in addition to the electron species to take into account all the plasma particle dynamics. The simulations results are summarized by Fig. 1, where the global structure of the bubble/blowout region is clearly observed in the electron density (Fig. 1a)).

It is also clear in Fig. 1, the high charge associated with the self-injected beams in this scenario, with the peak density of the injected beam more than 20 times higher than the background electron density. The radius of the bubble also agrees with the theoretical prediction ($r_{\text{bubble}} \approx 2\sqrt{a_0}c/\omega_p$ [5]). We note that for the time frame in Fig. 1, the laser pulse has undergone significant pulse compression and a_0 amplification [23], but it has not pump-depleted significantly. Fig. 1b) also illustrates the origin for the formation of monoenergetic beams, due to phase-space rotation [4,14], and the role of dephasing in limiting the maximum attainable energy of the accelerated electrons for ultra high intensities and high densities; in Fig. 1, the laser pulse has not been entirely depleted but the dephasing is already observable in the phase-space of the electrons. The simulation results show a total injected charge of 42 nC and a final peak energy of 2.3 GeV (42% of the electrons above 2.0 GeV), confirming the higher charge and lower final electron energy associated with this regime of ultra high laser intensities and high background plasma densities. We note that similar energy gains can be achieved with more moderate requirements in terms of the laser energy, as predicted in [5], and also observed in simulations of two-stage laser–plasma accelerators [24]. The overall efficiency of the acceleration process (23%) and the final energy (2.3 GeV) compare well with the theoretical predictions (19%, and 2.96 GeV) of the theoretical model in Ref. [21].

We note that Eqs. (1)–(4) are valid for the matched conditions, which are not met by the extreme blowout regime with $a_0 \gg 1$. The full phenomenological model in [5] can also be employed to obtain estimates in these conditions. Assuming that the laser pulse does not evolve, i.e. using the initial laser pulse parameters in the model in [5], the predicted energy gain is 1.7 GeV, and the predicted overall efficiency of the process is 11%. However, the simulations reveal that when the matched conditions are not met, strong pulse compression, self-focusing, and vector potential amplification are observed, as predicted in [23], and recently experimentally confirmed [25]. Thus, it is not possible to assume fixed laser parameters for these conditions. This is shown by the insert in Fig. 1b) which shows the Wigner transform of the laser pulse, denoting strong photon deceleration, and pulse compression. Assuming instead that the laser parameters are those measured after pulse compression and self-focusing ($a_0 \simeq 66$, pulse duration $\simeq 11$ fs, spot size $\simeq 6$ μm), the model of W. Lu et al. [5] predicts $E_{\max} = 2.1$ GeV and an overall efficiency of 21%, in very good agreement with the simulations. We note, however, that since the process and the dynamics in the extreme blowout regime are highly nonlinear, the theoretical models should be regarded as guidelines to the exploration of the conditions that lead to the optimization of the different scenarios.

In order to favor maximum energy gain, with lower self-injected charge, the second scenario must be considered, associated with the moderate blowout regime [5]. This scenario is obtained by decreasing the pulse intensity to an a_0 close to the self-guiding threshold ($a_0 \simeq 5.8$), through an increase of the laser duration to 110 fs, and the increase of the spot size to 50 μm, in order to guarantee the matched theoretical parameters (Eqs. (1), (2)). The theoretical model [5] predicts a monoenergetic bunch with a charge of ∼2 nC, and a maximum energy ∼12.9 GeV. To achieve these conditions, the optimal plasma density is 2.7×10^{17} cm^{-3}, and the acceleration length is 21.7 cm. These parameters were simulated both in QuickPIC and OSIRIS. In the QuickPIC simulations, we have also included radiation damping, and for the conditions in this paper we did not find significant differences between the simulation results.

For the QuickPIC simulations, the window size is $120 \times 700 \times 700$ μm^3, divided in $512 \times 256 \times 256$ cells. Since the quasi-static approximation does not include self-injection, a beam with 1.1×10^{-2} nC is placed at the back of the wake (in the region with highest accelerating gradients) with initial energy of 0.25 GeV, in order to mimic the main features of the self-injected beam. The electron beam has a Gaussian profile, $n_{\text{beam}} = n_{\text{beam0}} \exp(-r^2/2\sigma_r^2) \exp(-z^2/2\sigma_z^2)$, with radial/longitudinal width $\sigma_r = \sigma_z = 0.4c/\omega_{p0} = 4$ μm. We stress that the charge of the beam is low enough such that the beam does not perturb the wake, thus allowing us to understand the key properties of the accelerating structure in these moderate blowout conditions.

Fig. 2a) shows that the final energy agrees well with the theory, with a predicted accelerating gradient of 0.6 GeV/cm close to the accelerating gradient observed in the simulations of 0.8 GeV/cm. More important, we observe that the laser is effectively self-guided during the first half of the dephasing length. After ∼15 cm, the laser depletion to the plasma and the laser head erosion are too strong to guarantee self-guiding and the diffraction rate increases (Fig. 2b)), the wake structure deteriorates, impacting on the quality of the output beam. Furthermore, the final energy chirp (see Fig. 2c)) depends on the initial characteristics of the beam (position and energy chirp), which can be adjusted to obtain better quality output beams. Initial adjustments can also be made to emulate more closely the time evolution of the self-injection scenario, but we have observed that the quantitative features of the evolution of the peak energy of the beam remain unchanged. For externally injected beams, as discussed below, the beam charge

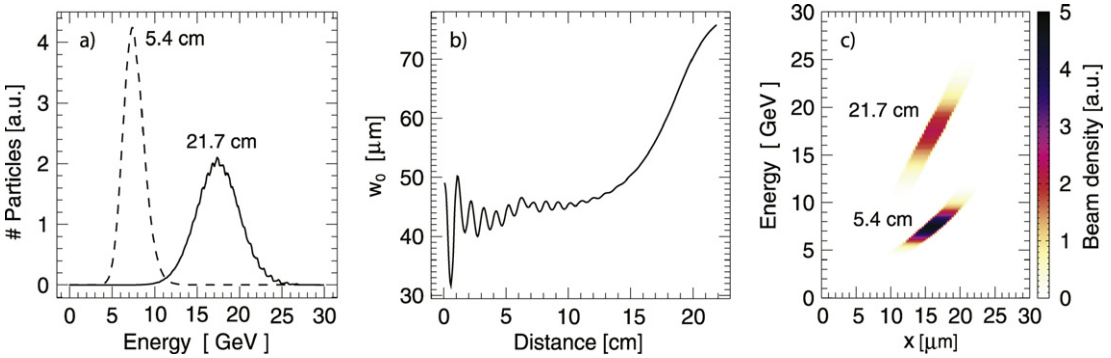

Fig. 2. QuickPIC simulations results for the conditions close to the self-guiding threshold in the moderate blowout regime: a) electron beam energy spectrum at 5.4 cm (dashed) and 21.7 cm (solid); b) laser spot size evolution with the propagation distance; c) phase-space of the electron beam for the same propagation distances considered in a).

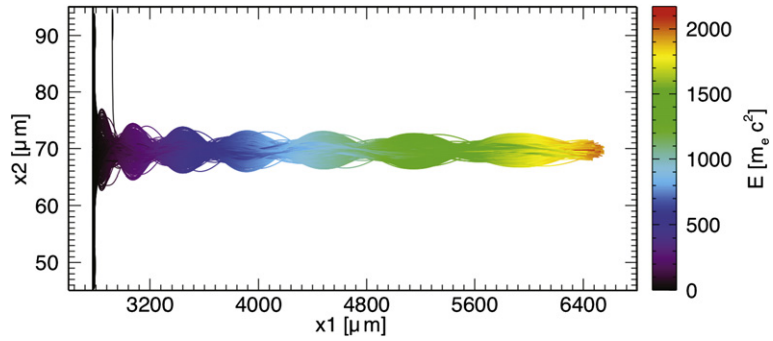

Fig. 3. Projection of the trajectories of the self-injected particles in the LWFA, moderate blowout regime. Injection occurs in the left-hand side of the visualization window. Most of the particles are injected off-axis. The particles move from left to right. The color in the trajectory represents the energy of the particle.

and the beam profile that guarantee optimal beam loading and the preservation of the properties of the injected bunch can be determined using the model recently presented in [26].

The same scenario was simulated with OSIRIS. The long plasma length (21.7 cm) required to achieve the maximum energy gain makes it impossible to perform a three-dimensional PIC simulation in the laboratory frame using the computational power currently available, since it would take more than 1 year in hundreds of processors to propagate the laser in such a long distance. In order to make this simulation feasible in OSIRIS, without resorting to approximations, we leveraged on the recently implemented boosted frame scheme [17,19], which strongly reduces computational requirements, by bringing together the relevant scales that it is necessary to numerically resolve (laser and plasma). The simulation was performed in a boosted Lorentz frame in a single day (512 CPU-cores), and confirmed the QuickPIC results, namely the possibility to achieve energies in excess of 10 GeV in the self-guiding/self-injection regime with the parameters associated with the second scenario. Furthermore, it was possible to observe that self-injection in these conditions also leads to phase-space rotation and the formation of quasi-monoenergetic beams [19].

Typical trajectories of the self-injected electrons are presented in Fig. 3, where it is clear the energy gain and the oscillations at the betatron frequency in the ion channel associated with the blowout region [27,28]. As the electrons oscillate, they will radiate. Estimates for the radiation in the 10 PW scenario, based on the post-processing of the tracks of the self-injected electrons extracted from the simulation, indicate an equivalent wiggler parameter for the betatron motion $K \gg 1$, with the total radiated energy reaching $\sim$80 mJ, the typical energy of the radiated photons in the 0.1–1 MeV range, and a beam divergence $\sim$2–5 mrad. A detailed discussion of the results in the boosted frame configuration will be presented in a future publication [19].

As conditions close to the energy frontier are approached, the radiation losses associated with the betatron motion of the electrons in the ion channel associated with the blowout region should be considered. The ratio between the energy loss due to the radiation and the energy gain in the accelerating field is $\Delta\gamma/\gamma \approx 3 \times$

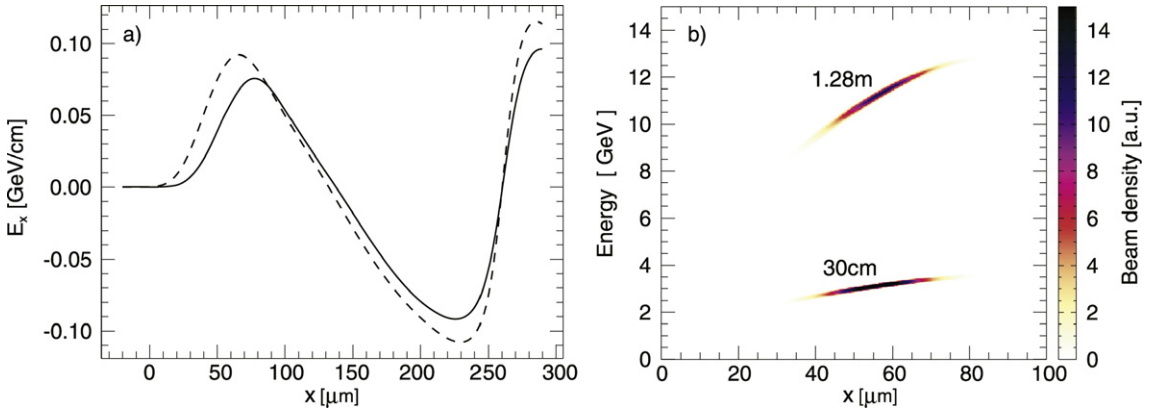

Fig. 4. QuickPIC results for the blowout regime with low intensity laser beam ($a_0 = 2$) for the parameters described in the main text: a) longitudinal electric field in the center of the simulation window after 30 cm (dashed) and 1.28 cm (solid); b) phase-space of the beam for the same propagation distances considered in a).

$10^{-5}\sigma_r^2[\mu\text{m}]E_b^2[50\ \text{GeV}]n_{\text{plasma}}^{3/2}[10^{16}\ \text{cm}^{-3}]/\epsilon_{\text{LW}}$ [5], where E_b is the energy of the beam, σ_r is the radius of the beam, and ϵ_{LW} is the normalized accelerating field. For the parameters considered in this paper $\Delta\gamma/\gamma \ll 1$. As observed in [5], as we approach the energy frontier it is critical to guarantee electron beams with $\sigma_r < 10$ μm such that $\Delta\gamma/\gamma \leqslant 10^{-2}$. For scenarios where radiation losses are important, numerical codes should include the radiation damping physics [29], as QuickPIC and Osiris already do.

3.2. External guiding and external injection

In the previous scenarios, higher intensities were explored. For such intensities, the laser pulse can be self-guided since the electron density depression associated with the blowout region can self-guide the back of the laser pulse, while the front of the pulse erodes/pump-depletes faster than it diffracts [5]. The self-guiding regime has been recently experimentally demonstrated [13]. These scenarios require high intensities ($a_0 \geqslant 5.8$). However, if external guiding can be achieved, e.g. by a proper tailoring of the plasma (plasma channel), and an externally injected beam can be synchronized with the accelerating structure, the requirements for the laser intensity can be relaxed, and lower intensities can be considered, thus increasing the conversion efficiency from the laser energy to the accelerated electrons, and the maximum energy gain (cf. Eq. (5)).

The matched conditions for the pulse duration, plasma density, and laser spot size change accordingly. For a lower intensity blowout regime [5] with $a_0 = 2$, the matched laser pulse duration is 224 fs, and the laser spot size is 101 μm. The matched plasma density is $n_0 = 2.2 \times 10^{16}\ \text{cm}^{-3}$, and a channel must be used to guide the laser through an accelerating length of 5.28 m. We have modeled this scenario with QuickPIC, with a simulation window with $310 \times 1400 \times 1400\ \mu\text{m}^3$ divided in $1024 \times 128 \times 128$ cells. The channel parameters follow the standard theory to guarantee matched propagation [3], with a radial density profile $n(r) = n_0(1 + 0.0465(rc/\omega_{p0})^2) = n_0(1 + 3.8 \times 10^{-5}r^2[\mu\text{m}]$ up to $r = 7.14c/\omega_{p0} = 250$ μm, and then linearly decreasing, down to 0, up to $r = 48.5c/\omega_{p0} = 1.7$ mm. The electron beam has a Gaussian profile, both longitudinally and transversally, with radial/longitudinal width $\sigma_r = \sigma_z = 0.4c/\omega_{p0} = 4$ μm, with a total charge of 1.1×10^{-3} nC. Fig. 4 summarizes the main results, demonstrating the stability of the accelerating structure, and the steady acceleration of the external beam in the wakefield structure generated with the more moderate intensities.

The simulations for this range of parameters show clearly the effect of the channel in providing an extremely stable laser propagation and wake excitation, creating the perfect conditions for particle acceleration for distances in excess of 1 meter. The accelerating gradient (90 MeV/cm) is in good agreement with the theoretical predictions (100 MeV/cm), leading to the expected bunch energy after 1.28 m propagation (∼13 GeV). These results indicate that, after 5.28 m of propagation in the channel, an energy of +50 GeV can be achieved. These results will be fully explored elsewhere. We have also performed simulations with electron beams with the total charge/beam profile determined by the theory for beam loading in the nonlinear blowout regime [26], and we have found the same quantitative behavior. Furthermore, for injected beams with the charge and beam profile determined according to [26] we have observed the

conservation of the emittance of the beam and of the energy spread, clearly demonstrating the excellent accelerating properties of the bubble.

4. Conclusions and prospects

We have explored the prospects for electron acceleration with the next generation of laser systems, which will be operating in the 10 PW range. The available energy in these systems will allow for scenarios with ultra-relativistic laser intensities or with moderate intensities, probing and exploring a large parameter space in terms of laser parameters (e.g. the pulse duration and the laser spot size). Thus, the possibility to identify the optimal conditions for electron acceleration, and the optimized monoenergetic beam parameters will be possible, provided that full control over the focusing optics, pulse duration and wavefront profile is possible. Recent experiments indicate that such control is indeed possible [30,31], and can provide fine tuning over the features of the beams injected in the blowout regime.

The theoretical scalings and the results of numerical simulations for the next generation of laser systems demonstrate that very high charge multi-GeV electron beams can be generated at ultra-high intensities. On the other hand, if moderate intensities are considered the charge in the self-injected beam can still be high ($\sim$2 nC), and the energy of the electron beam can be in excess of 10 GeV. If further control over the plasma source (e.g. with a plasma channel) is possible, providing a guiding mechanism for $a_0 \simeq 2$, then stable guiding and acceleration can be achieved over distances on the meter-scale opening the possibility to the generation of electron beams with energies close to the energy frontier. These results have been confirmed with reduced models (QuickPIC) and with full-scale simulations (OSIRIS). All approaches seem to provide a consistent direction to achieve multi GeV self-injected beams in LWFA, either favoring ultra high charge electron beams, or favoring $+10$ GeV/$+50$ GeV self-injected/externally injected electron beams in a single LWFA stage.

As the prospects to reach energies close to the energy frontier become realistic, other beam parameters should also be addressed. The field structure associated with the blowout regime has excellent properties (high gradient, radially independent acceleration fields for electrons, linear focusing radial fields) [20,32], as demonstrated by the experimental results at SLAC with electron beam drivers (e.g. [33]). Either by using specially tailored externally injected electron beams, that guarantee the proper beam loading of the bubble [26], or by using ultra-short externally injected beams, produced by conventional accelerator technology or by all-optical mechanisms [34–37], the energy spread of the injected beam can be maintained. Moreover, the beam can be transported with minimum transverse-profile modifications [32].

Several developments should be in place to take full advantage of the possibilities opened by these laser systems. First of all, the new regimes will require a new generation of plasma sources with low density, guiding properties, and considerably longer scale lengths (up to several meters). Secondly, a fine control over the focusing properties of the laser beams will be required, in order to operate in the optimal conditions for (self)-guided propagation. Finally, the ability to inject high quality electron beams, either from an external accelerator or from an all-optical injection scheme, as recently demonstrated [36], is critical to take full advantage of the accelerating properties of the bubble in the blowout regime. If these challenges can be overcome, the prospects to generate electron beams with unprecedented characteristics (in terms of energy, charge, and duration) will be within reach of the next generation of ultra intense lasers in the 10 PW range.

Acknowledgements

The authors would like to thank Drs. Peter Norreys and Raoul Trines for the discussions that triggered this work. This work was partially supported by Fundação para a Ciência e Tecnologia (Portugal), and by the European Community – New and Emerging Science and Technology Activity under the FP6 “Structuring the European Research Area” programme (project EuroLeap, contract number 028514). The simulations presented here were produced using the IST Cluster (IST/Portugal), the Dawson cluster (UCLA) and the Franklin supercomputer (NERSC).

References

[1] http://www.clf.rl.ac.uk/Facilities/vulcan/index.htm.
[2] T. Tajima, J.M. Dawson, Phys. Rev. Lett. 43 (1979) 267.

[3] E. Esarey, et al., IEEE Trans. Plasma Sci. 24 (1996) 252, and references therein.
[4] A. Pukhov, J. Meyer-ter-Vehn, Appl. Phys. B: Lasers Opt. 74 (2002) 355.
[5] W. Lu, et al., Phys. Rev. ST Accel. Beams 10 (2007) 061301.
[6] R.A. Fonseca, et al., Plasma Phys. Controlled Fusion 50 (2008) 124034.
[7] R.A. Fonseca, et al., Lecture Notes in Computer Science, vol. 2329, Springer-Verlag, 2002, III-342.
[8] C. Huang, et al., J. Comp. Phys. 217 (2006) 658.
[9] S.P.D. Mangles, et al., Nature 431 (2004) 535;
C.G.R. Geddes, et al., Nature 431 (2004) 538;
J. Faure, et al., Nature 431 (2004) 541.
[10] W.P. Leemans, et al., Nat. Phys. 2 (2006) 696.
[11] S. Karsch, et al., New J. Phys. 9 (2007) 415.
[12] N.A.M. Hafz, et al., Nat. Photonics 2 (2008) 571.
[13] S. Kneip, S.R. Nagel, S. Martins, et al., submitted for publication (2009).
[14] F.S. Tsung, et al., Phys. Rev. Lett. 93 (2004) 185002.
[15] T.A. Antonsen Jr., P. Mora, Phys. Rev. Lett. 69 (1992) 2204.
[16] P. Sprangle, E. Esarey, A. Ting, Phys. Rev. Lett. 64 (1990) 2011.
[17] J.-L. Vay, Phys. Rev. Lett. 98 (2007) 130405.
[18] P. Abreu, R.A. Fonseca, L.O. Silva, AIP Conf. Proc. 1086 (2009) 328.
[19] S.F. Martins, et al., in preparation (2009).
[20] W. Lu, et al., Phys. Rev. Lett. 96 (2006) 165002.
[21] S. Gordienko, A. Pukhov, Phys. Plasmas 12 (2005) 043109.
[22] S.P.D. Mangles, et al., Phys. Plasmas 14 (2007) 056702.
[23] F.S. Tsung, et al., Proc. Natl. Acad. Sci. USA 99 (2002) 29.
[24] V. Malka, et al., Phys. Rev. STAB 9 (2006) 091301.
[25] J. Faure, et al., Phys. Rev. Lett. 95 (2005) 205003.
[26] M. Tzoufras, et al., Phys. Rev. Lett. 101 (2008) 145002.
[27] D.H. Whittum, A.M. Sessler, J.M. Dawson, Phys. Rev. Lett. 64 (1990) 2511.
[28] S. Kneip, S.R. Nagel, C. Bellei, et al., Phys. Rev. Lett. 100 (2008) 105006.
[29] S. Kiselev, et al., Phys. Rev. Lett. 93 (2004) 135001.
[30] Y. Glinec, et al., EPL 81 (2008) 64001.
[31] A. Popp, et al., presented at Advanced Accelerators Concepts Workshop 2008.
[32] J.B. Rosenzweig, et al., Phys. Rev. A 44 (1991) R6189.
[33] I. Blumenfeld, et al., Nature 445 (2007) 741.
[34] D. Umstadter, J.-K. Kim, E. Dodd, Phys. Rev. Lett. 76 (1996) 2073.
[35] E. Esarey, et al., Phys. Rev. Lett. 79 (1997) 2682.
[36] J. Faure, et al., Nature 444 (2006) 737.
[37] K. Schmid, et al., Phys. Rev. Lett. 102 (2009) 124801.